Inorganica Chimica Acta, *178* (1990) 151–163

Coordination of the strong field di-imine 3,3′-bipyridazine. Structural, magnetic and spectroscopic properties of the Fe(II), Co(II) and Ni(II) complexes

Djulia Onggo, A. David Rae* and Harold A. Goodwin*

School of Chemistry, University of New South Wales, P.O. Box 1, Kensington, NSW 2033 (Australia)

(Received May 16, 1990)

Abstract

The di-imine system 3,3′-bipyridazine (L) generates a particularly strong ligand field and this is revealed in the low-spin nature of $[FeL_2(NCS)_2]$ and of salts of $[FeL_3]^{2+}$, the appearance of a doublet ⇄ quartet transition in $[CoL_3]^{2+}$, and the high energy (13 200 cm^{-1}) of the $^3A_{2g} \rightarrow {}^3T_{2g}$ transition in the electronic spectrum of $[NiL_3]^{2+}$. In attempts to prepare bis(ligand) complexes the mixed low-spin cationic, high-spin anionic complexes $[FeL_3][FeCl_4]$, $[FeL_3][Fe(NCS)_4]$ and $[FeL_3][FeCl_4]_2$ were isolated. These were characterised by magnetic and Mössbauer spectral measurements. The structures of both $[FeL_3][ClO_4]_2$ and $[NiL_3][ClO_4]_2$ reveal unusually short Fe–N (1.927(3) Å) and Ni–N (2.060 Å) distances and these, and the high field strength, are believed to result in part from the absence of *ortho*-hydrogen atoms in the ligand molecules which cause considerable inter-ligand repulsion in complexes of the related di-imine, 2,2′-bipyridine. $[FeL_3][ClO_4]_2$ crystallises in space group $P\bar{3}c1$ ($Z=2$) with cell parameters $a=10.281(2)$, $b=10.281(2)$, $c=15.863(4)$ Å. A total of 430 reflections with $I_o > 3\sigma(I_o)$ was observed and a final value of $R=0.045$ was obtained. $[NiL_3][ClO_4]_2$ crystallises in space group $P321$ ($Z=1$) with cell parameters $a=10.225(3)$, $b=10.225(3)$, $c=8.049(3)$ Å. Stacking faults and twinning create an apparent $P\bar{6}2c$ diffraction symmetry. A total of 266 reflections with $I_o > 3\sigma(I_o)$ was observed and a final value of $R=0.042$ was obtained.

Introduction

One of the features of the coordination of the strong field bidentate ligand 2,2′-bipyridine is the presence of inter-ligand repulsions that are set up in complexes through steric interactions involving the 6- and 6′-hydrogen atoms (**1**). This interaction is very pronounced when two molecules of the base coordinate in a plane and in fact this mode of coordination rarely occurs, bis-ligand four-coordinate complexes generally being distorted towards a tetrahedral geometry and bis(ligand) six-coordinate complexes adopting a *cis*-octahedral configuration [1], though *trans* species are known [2]. Even in tris(ligand) octahedral complexes there is evidence for these inter-ligand interactions and they are manifested in a trigonal twist angle closer to the octahedral value than is predicted by theory [3]. In the related di-imine system 3,3′-bipyridazine (**2**) (abbreviated L in formulae below) the presence of the nitrogen atoms in the corresponding positions may well be expected to reduce these inter-ligand steric repulsions, although lone electron pair interactions could play a similar role.

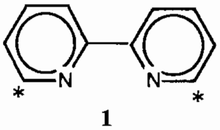

1

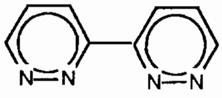

2

3,3′-Bipyridazine was described in 1967 by Lafferty and Case [4] who noted that it gave a ferroin test. The $[FeL_3]^{2+}$ cation was subsequently investigated by Gillard *et al.* [5] who observed a negligible rate of dissociation in water and an unusually slow rate for hydroxide ion attack for it. The recent studies of Ernst and Kaim [6] have revealed strong back-bonding ability for this ligand system, arising from the synergistic effect of a surprisingly high base strength.

The present study was undertaken primarily to characterise the complex $[FeL_3]^{2+}$ and to investigate the possibility of two molecules of L coordinating in a plane, leading to *trans* structures for complexes of the type $[FeL_2X_2]$. We find L to be a very strong field ligand which confers a marked stabilisation of

---

*Authors to whom correspondence should be addressed.

0020-1693/90/$3.50

iron(II) in the tris(ligand) complex, the formation of bis(ligand) complexes being resisted.

Experimental

Preparation of 3,3'-bipyridazine (2)

3,3'-Bipyridazine was prepared initially by literature methods [4, 7, 8]. However, the yield was always found to be unacceptably low. By application of the recently described [9] use of the nickel(0) complex of triphenylphosphine as a coupling reagent, 3-chloropyridazine could be converted to 3,3'-bipyridazine in reasonable yield (40–50%). The overall preparative procedure involved the initial synthesis of 1,4,5,6-tetrahydro-6-oxopyridazine-3-carboxylic acid [10] from α-keto-glutaric acid followed by conversion to 1,6-dihydro-6-oxopyridazine-3-carboxylic acid which was subsequently decarboxylated to 3-pyridazinone. This was then converted to 3-chloropyridazine [11] and then finally the coupling reaction was applied to yield bipyridazine. The details of this are given in the following. To a mixture of $NiCl_2 \cdot 6H_2O$ (4.72 g), triphenylphosphine (20.8 g) and zinc powder (1.28 g) in dry dimethylformamide (100 ml) under nitrogen at 70 °C for 1 h, 3-chloropyridazine (2.5 g) was added with rapid stirring. The stirring was continued for 5 h and the mixture was then poured into a solution of concentrated aqueous ammonia (200 ml). The solution was extracted with chloroform (3 × 100 ml), the chloroform extracts were combined and dried with sodium sulfate. The solvent was removed by distillation and the residue was extracted with hydrochloric acid (1 M). After neutralisation with sodium hydroxide, the mixture was extracted again with chloroform. After evaporation of the solvent, white crystals were obtained, m.p. 230–232 °C (lit. [4] 224–226 °C). *Anal.* Found: C, 60.6; H, 3.7; N, 35.2. Calc. for $C_8H_6N_4$: C, 60.8; H, 3.8; N, 35.4%.

Preparation of complexes

All iron complexes were prepared under an atmosphere of nitrogen.

$[ML_3]X_2$ (M = Fe, Co, Ni; X = ClO_4, BF_4)

To a warm solution of free ligand **2** (3 mmol) in ethanol (approx. 10 ml) was added a warm solution of $M[ClO_4]_2 \cdot 6H_2O$ or $M[BF_4]_2 \cdot 6H_2O$ (M = Fe, Co, Ni) (1 × mmol) in ethanol (approx. 5 ml). The complex salt was generally induced to crystallise directly. The products were washed with a little ethanol and dried in vacuum over P_2O_5.

$[FeL_3][FeCl_4]$

To a well stirred solution of iron(II) chloride tetrahydrate (0.13 g) in ethanol (5 ml) was added **2** (0.2 g) in ethanol (10 ml). The deep red complex $[FeL_3][FeCl_4]$ crystallised. It was washed with ethanol and dried over P_2O_5 in vacuum.

$[FeL_3][Fe(NCS)_4]$

Iron(II) chloride tetrahydrate (0.15 g) and **2** (0.4 g) were mixed in warm water (15 ml) and then a solution of KNCS (1 g) in water (5 ml) was added. The red complex $[FeL_3][NCS]_2$ crystallised. This was washed with ethanol and dried over P_2O_5 in vacuum. It was then refluxed with acetone (60 ml) for 20 h when it was converted to $[FeL_3][Fe(NCS)_4]$. This product was washed several times with acetone and dried over P_2O_5 in vacuum.

$[FeL_3][FeCl_4]_2$

To a solution of iron(III) chloride (0.24 g) in hot ethanol (10 ml) was added a solution of **2** in ethanol (5 ml). The deep red product crystallised immediately. It was washed with ethanol and dried over P_2O_5 in vacuum.

$[FeL_2(NCS)_2]$

To a well stirred solution of iron(II) chloride tetrahydrate (0.2 g) was added a solution of potassium thiocyanate (0.2 g) both in dry methanol (10 ml) at room temperature. After the iron(II) thiocyanate was completely formed, the precipitated potassium chloride was filtered off. To the filtrate, a stoicheiometric amount of 3,3'-bipyridazine (0.3 g) in methanol (10 ml) was added dropwise whereupon the complex crystallised. The product was collected, washed with methanol and dried over P_2O_5 in vacuum.

Magnetic measurements

The magnetic data for solid samples were obtained using a Newport variable temperature Gouy balance calibrated with $CoHg(NCS)_4$. All data have been corrected for diamagnetism calculated using Pascal's constants [12]. Curie–Weiss θ values refer to the expression $\chi_M = C/(T-\theta)$ and were obtained from an extrapolation of a linear least-squares plot of $1/\chi_M$ against T. Molar susceptibilities (χ_M) are quoted in $m^3\ mol^{-1}$ and the magnetic moments were calculated according to the relationship $\mu = 798(\chi_M T)^{1/2}$. Magnetic data for samples in solution were obtained using a Bruker CXP 300 NMR spectrometer according to the Evans method [13]. Since this instrument utilises a superconducting magnet the modification of the Evans method as given by Baker *et al.* [14] was followed.

Mössbauer spectra

Mössbauer spectra were recorded with a conventional spectrometer utilising a Wissel drive unit and a Norland multichannel analyser. The source used was ^{57}Co in a palladium matrix. The temperature of the absorber was maintained to within ±1° of the set temperature in a custom made cryostat. The velocity scale was calibrated against iron foil and sodium nitroprusside. The isomer shifts quoted are relative to the mid point of the iron spectrum at room temperature. Mössbauer spectral parameters were extracted from a least-squares fit of the data to Lorentzian line shapes.

Electronic spectra

Electronic spectra were recorded on a Zeiss PMQ II spectrophotometer equipped with a diffuse reflectance accessory calibrated against magnesium oxide. For variable temperature measurements a special brass attachment with silica glass windows was used. For low temperatures the fitting was sealed and a stream of cold nitrogen gas was passed over the assembly to prevent condensation. The fitting was then place in contact with the base of an insulated brass dewar filled with liquid nitrogen, or, at elevated temperatures silicone oil held at a fixed temperature.

Infrared spectral data

Infrared spectra were measured for samples as mulls in paraffin or halocarbon with a Perkin-Elmer PE 580B instrument.

Cyclic voltammetry

The cyclic voltammograms for $[FeL_3][ClO_4]_2$ were obtained with a PAR 173/175 system. A 10^{-3} M solution of the complex was utilised in a cell fitted with a platinum working electrode, a SCE as reference electrode and a platinum counter electrode.

Analytical data

Satisfactory analyses for carbon, hydrogen, nitrogen and metal were obtained for all complex samples (see 'Supplementary material'). The C, H and N analyses were carried out by Dr H. Pham, School of Chemistry, University of New South Wales. The metal content of the complexes was estimated by gravimetric and ICP methods.

Crystallographic analysis

Crystals of $[FeL_3][ClO_4]_2$ were grown from acetone/petroleum ether (40–60°) mixture and those of $[NiL_3][ClO_4]_2$ were grown from aqueous acetone.

Data collection

The reflection data were measured with an Enraf-Nonius CAD-4 diffractometer in $\theta/2\theta$ scan mode using graphite monochromatised molybdenum radiation ($\lambda = 0.7107$ Å). Data were corrected for absorption. Reflections with $I_o > 3\sigma(I_o)$ were considered observed. Reflection weights used were $1/\sigma^2(F_o)$, with $\sigma(F_o)$ being derived from $[\sigma^2(I_o) + (0.04I_o)^2]^{1/2}$. The weighted residual is defined as $R_w = (\Sigma w(\Delta F)^2/\Sigma wF_o^2)^{1/2}$. Atomic scattering factors and anomalous dispersion parameters were from International Tables for X-ray Crystallography [15]. Structure solution was by MULTAN80 [16] and refinement used RAELS [17]. ORTEP-II [18] was used for the preparation of the structural diagrams and an IBM 3090 computer was used for all calculations. The crystal data for the complexes are listed in Table 1.

Determination and refinement of the structure of $[NiL_3][ClO_4]_2$

The diffraction pattern had the intensity distribution and systematic absences consistent with space groups $P\bar{6}2c$ (No. 190) and $P6_3/mmc$ (No. 194), viz. $F(hhl) = 0$ if l is odd. However since $Z = 1$ and 32 point symmetry is expected for the cation twinning and/or disorder was suspected. The Patterson map showed peaks consistent with a Ni atom disordered between 0,0,0 and 0,0,$\frac{1}{2}$ and Cl atoms at $\frac{1}{3},\frac{2}{3},\frac{1}{4}$ and $\frac{2}{3},\frac{1}{3},\frac{3}{4}$ consistent with space group $P6_3/mmc$ and its subgroups $P\bar{6}2c$ and $P321$ (No. 150), the latter being the expected symmetry of an ordered structure. A map of $P6_3/mmc$ symmetry phased from such a model located the coordinated N atoms at (12 (k) m) $2x$, x, z with $x = 0.10$ and $z = 0.14$. Now $P6_3/mmc$ is made up of the product of symmetry elements of the

TABLE 1. Crystallographic details for bpdz compounds

Compound	$[Fe(C_8H_6N_4)_3][ClO_4]_2$	$[Ni(C_8H_6N_4)_3][ClO_4]_2$
Molecular weight	729.2	732.1
Crystal class	hexagonal prism	hexagonal prism
Space group	$P\bar{3}c1$ (No. 165)	$P321$ (No. 150)
Z	2	1
a (Å)	10.281(2)	10.225(3)
b (Å)	10.281(2)	10.225(3)
c (Å)	15.863(4)	8.047(3)
α (°)	90	90
β (°)	90	90
γ (°)	120	120
V (Å^3)	1452.1(4)	728.8(3)
ρ_c (g cm^{-3})	1.67	1.67
Radiation	Mo Kα	Mo Kα
μ (cm^{-1})	7.7	9.2.
λ (Å)	0.7107	0.7107
No. unique reflections	633	382
No. observed reflections	430	266
Final R	0.045	0.042
Final R_w	0.048	0.043

ordered structure $P321$ and symmetry elements (x, y, z; x, y, $\frac{1}{2}-z$; $-x$, $-y$, $-z$; $-x$, $-y$, $\frac{1}{2}+z$) of $P2_1/m$ which describe possible disorder and/or twinning rules. It was decided to initially restrict the twin/disorder rule to x, y, $\frac{1}{2}-z$ as this leaves the projection down c of the structure the same as for an ordered structure whereas the other possible operations do not. The centres of the ligand six-membered rings and the anions lie on the disordering plane at $z=\pm\frac{1}{4}$ and it is assumed that columns of cations parallel to c are ordered but the equal probability of the two chiralities of the cation causes $P\bar{6}2m$ diffraction symmetry assuming Friedel's law does not hold because of anomalous scattering factors.

The expectation value of the observation $I(hkl)$ can be expressed in terms of the structure factor $F(hkl)$ of an ordered $P321$ structure $\rho(x, y, z)$ as

$$\begin{aligned} I(hkl) &= \langle|(1-\alpha)F(hkl)+(-1)^l\alpha F(hk-l)|^2\rangle \\ &= \langle|F_1(hkl)+(1-2\alpha)F_2(hkl)|^2\rangle \\ &= |F_1(hkl)|^2+\langle(1-2\alpha)^2\rangle|F_2(hkl)|^2 \\ &\quad +\langle(1-2\alpha)\rangle[F_1(hkl)F_2(hkl)^*+F_1(hkl)^*F_2(hkl)] \end{aligned}$$

where $\alpha/(1-\alpha)$ is the disorder ratio in individual mosaic blocks and $F_1(hkl)=[F(hkl)+(-1)^lF(hk-l)]/2$, $F_2(\mathrm{hkl})=[F(hkl)-(-1)^lF(hk-l)]/2|F_1(hkl)|^2$ and $|F_2(hkl)|^2$ each have $P\bar{6}2m$ diffraction symmetry. $[F_1(hkl)F_2(hkl)^*+F_1(hkl)^*F_2(hkl)]$ can be reexpressed as $[|F(hkl)|^2-|F(hk-l)|^2]/2$ and would create $P321$ diffraction symmetry if $\langle(1-2\alpha)\rangle\neq 0$. The diffraction pattern thus has $P\bar{6}2m$ symmetry if $\langle\alpha\rangle=1/2$. $I(hkl)=|F_1(hkl)|^2+|F_2(hkl)|^2$ if a 1:1 twinning of ordered mosaics exists, i.e. $\alpha=0$ and 1 only with equal probability. However $I(hkl)=|F_1(hkl)|^2+\langle(1-2\alpha)^2\rangle|F_2(hkl)|^2$ if α is spread about a mean value of $\frac{1}{2}$. Averaging $I(hkl)$ and $I(hk-l)$ data makes $I(hkl)=|F_1(hkl)|^2+\langle(1-2\alpha)^2\rangle|F_2(hkl)|^2$ exactly and $\langle(1-2\alpha)^2\rangle=0$ only if all mosaics are randomly disordered with $\alpha=\frac{1}{2}$.

Now $F(hkl)=F(hk-l)$ when $h=k$ and we see that $I(hhl)=|F_1(hhl)|^2$ when l is even and $I(hhl)=\langle(1-2\alpha)^2\rangle|F_2(hhl)|^2$ when l is odd. An apparent systematic absence is created if α is not widely distributed about $\frac{1}{2}$. For example if α has values of 0.45 and 0.55 with equal probability of $\frac{1}{2}$ then $\langle(1-2\alpha)^2\rangle=0.01$. The Ni atom at the origin contributes to only $F_1(hkl)$ when l is even and to only $F_2(hkl)$ when l is odd and for a sufficiently large number of observed reflections (particularly the weaker l odd reflections) the ratio $\langle(1-2\alpha)^2\rangle|F_2(hkl)|^2/|F_1(hkl)|^2$ is sufficiently large for α to be refinable even when $\langle(1-2\alpha)^2\rangle$ is about 0.01. It should be noted that the refinement of atomic parameters is dominated by the $F_1(hkl)$ component of the data and consequently $F_2(hkl)$ is essentially determined by the refinement of $F_1(hkl)$ which is the Fourier transform of the disordered structure $\rho_1(x, y, z)=[\rho(x, y, z)+\rho(x, y, \frac{1}{2}-z)]/2$. $F_2(hkl)$ is the Fourier transform of $\rho_2(x, y, z)=[\rho(x, y, z)-\rho(x, y, \frac{1}{2}-z)]/2$.

Different locations for the bidentate ligand are possible but these only distinguish orientations of $P321$ in a $P6/mmm$ lattice. The asymmetric unit of $P321$ contains one six-membered ring of the bidentate ligand which was incorporated into the structure using a model in which the two rings of the bidentate ligand and the Ni atom were coplanar and the coordinated N atom coincided with a peak found on a $P6_3/mmc$ Fourier phased from the Ni and Cl atoms. A further map of $P\bar{6}2c$ symmetry located the O atoms.

Refinement of the structure was carried out using the comprehensive constrained least-squares refinement program RAELS. Refinable local coordinates (X, Y, 0) for the coplanar atoms of the ring were defined relative to a refinable local orthonormal axial system and produced a model with sufficient degrees of freedom to describe reality. The origin of the axial system was constrained to move along the a axis of symmetry 2. By fixing at $X=0$ the local coordinate for C(4), rotation about the local Y axis constitutes a twist of one ligand ring relative to the other about the C(4)–C(4)′ bond while keeping this bond and the ring coplanar. Rotation about the local X axis then sets the pitch of the ligand propellor. Rotation about the local Z axis was not refined as this is a redundant parameter. Thus fourteen refined parameters describe the atomic positions of the cation. Hydrogen atoms were given sensible positions in each refinement cycle but were not refined. Nine refinable rigid body thermal parameters were used to describe the thermal motion of the ligand, being those TLX parameters consistent with the local twofold symmetry of the bidentate ligand. The ClO_4^- ion lies on a threefold axis and because of the overlap of Cl and O atoms related by the disordering mirror plane perpendicular to c the anion was constrained to be a perfect tetrahedron and so atom positions were described by three variables defining the size, orientation and position. Those five TLX variable parameters consistent with the local threefold symmetry were used to describe the thermal motion [19]. Two anisotropic thermal parameters describe the Ni atom.

The initial refinement model used four equal twin components $F(hkl)$, $F(hk-l)$, $F(-h-kl)$ and $F(-h-k-l)$ for data merged under $P321$ symmetry. The symmetry was reduced to $P321$ by using a 0.6:0.4 occupancy ratio for the cations. The correlation of these occupancies with the ClO_4^- occupancies was resolved by refinement of the latter away from an initial 0.5:0.5 model. The refined occupancy ratios were then constrained to be the same for cation and anion in all subsequent refinement cycles. At the conclusion of refinement a further cycle with cation/anion occupancy ratios uncoupled showed that the assumed model was justified as shifts of less than half a standard deviation resulted. Refinement of the amounts of the four twin components showed the $F(-h-kl)$ and $F(-h-k-l)$ components to be absent and the $F(hkl)$ and $F(hk-l)$ components to be effectively equal. Merge statistics were effectively the same for $P3$, $P321$ and $P\bar{6}2m$ but 1% worse for $P6/mmm$. Consequently data were merged under $P\bar{6}2m$ diffraction symmetry for further refinement. Using a 1:1 twinning model a final value of $\alpha = 0.555(3)$ was obtained implying $\langle(1-2\alpha)^2\rangle = 0.0121(13)$. In the data merging the variance of the mean of any set of N observations was chosen as the greater of $\Sigma(I-\Sigma I/N)^2/N(N-1)$ and the counting statistics estimate.

It is interesting to note that for the ClO_4^- anion the libration parameter $L_{11} = L_{22} = 0.116(5)$ is much bigger than $L_{33} = 0.007(1)$ radians^2 which supports the twinning disorder mechanism proposed, viz. the structure looks perfectly ordered in projection down c but some columns of cations have one chirality and some have the opposite chirality. These two types of columns are related by glide planes at $z = \pm\frac{1}{4}$. The large L_{11} parameter is evidence of the anions accommodating the requirements of being a buffer between columns of opposite chirality as threefold axis related O atoms try to be at different z heights. A final value of $R = 0.0426$ was obtained for the 266 independent reflections considered observed $(I > 3\sigma(I))$. A final refinement cycle starting from the correct model but with $\Delta f''$ changed to $-\Delta f''$ gave $R = 0.0514$. A final refinement cycle starting from the correct model but with $\langle(1-2\alpha)^2\rangle = 0.0$ gave $R = 0.0439$. The refinability of $\langle(1-2\alpha)^2\rangle$ is better illustrated by $s = 1.264$ compared to $s = 1.301$ and by the value of $R = 0.0624$ compared to 0.0649 for the 90 observed reflections with l odd and $\sin\theta/\lambda > 0.2$.

Determination and refinement of structure of $[FeL_3][ClO_4]_2$

The diffraction pattern had the intensity distribution and systematic absences consistent with space groups $P3c1$ (No. 158) and $P\bar{3}c1$ (No. 165), viz. $F(h0l) = 0$ if l is odd. Since $Z = 2$ and 32 point symmetry is expected for the cation the centrosymmetric space group $P\bar{3}c1$ (No. 165) was chosen and locates Fe atoms at the 32 site $0, 0, \pm\frac{1}{4}$. Only $l = 2n$ data are phased by these atoms. A Fourier map using only these data produces a disordered picture of the structure as atoms are seen at both $\boldsymbol{r}$ and $\boldsymbol{r} + 1/2\boldsymbol{c}$. By selecting one of two possible orientations of the ligand, one selects between alternative origins $1/2c$ apart and creates an initial phase estimate of l odd data. The Cl atoms were then correctly located using the resulting Fourier map. A subsequent difference map located the O atoms. Refinement of the structure was carried out using the comprehensive constrained least-squares refinement program RAELS. Choice of axis system was made so that the parameterisation used for the cation of the Ni analogue was transferable to the Fe complex by a simple $1/2c$ translation. The ClO_4^- ion lies approximately on a threefold axis and consequently space group symmetry imposes threefold disordering about this axis. The Cl and O atoms were constrained to form a perfect tetrahedral anion and so atom positions were described by thirteen variables defining the size, orientation and position. Those five TLX variable parameters consistent with the local threefold symmetry were used to describe the thermal motion. Two anisotropic thermal parameters describe the Fe atom. Difference maps located a further orientation of the ClO_4^- ion. The final model for this ion was therefore expanded by seven more parameters defining relative occupancy, 0.908(12):0.098 and a second orientation and origin. The same TLX parameters and internal coordinates of refinable bond length were used for both oriented fragments. Back Fourier transform calculations [20] showed that this was sufficient parameterisation to make the residual error in the region of the electron density map no different to that in other regions of the map. A final value of $R = 0.045$ was obtained for the 430 reflections considered observed $(I > 3\sigma(I))$. Data with l odd are systematically weak since they contain no contribution from the Fe atom.

Comparison of the Fe and Ni structures

Crystals of the Fe and Ni complexes have similar a and b axes but the c axis for the Fe complex $(Z = 2)$ is approximately twice that of the Ni complex $(Z = 1)$. Volume ratio = 1.992(1). Comparison of the asymmetric units for the two complexes can be made making a transformation between x, y, z of the Fe complex and x', y', z' of the Ni complex, viz. $x = x'$, $y = y'$, $z = 0.25 + 0.5\ z'$.

The cation positions in each structure are essentially superimposed by the transformation. The disordered ClO_4^- ion at $\frac{2}{3}, \frac{1}{3}, \frac{3}{4}$ (equivalent position of $\frac{1}{3}, \frac{2}{3}, \frac{1}{4}$) in the Ni complex becomes a disordered ClO_4^- ion at $\frac{2}{3}, \frac{1}{3}, \frac{5}{8}$ in the Fe complex. Consequently, in terms of the distribution of point charges, the two structures are essentially identical.

For both compounds, the cations are ordered within columns parallel to the c axis. In the Fe case no disordering of cations was observed while in the Ni case the observed disorder creates an apparent separation of Ni atoms of just 4 Å, causing impossible overlap of molecules. The disordering must therefore be between columns, not within columns. In the Fe case the adjacent cations in the column are related by c glide operations while in the Ni case they are related by pure translation. It would appear that the environment of the anion determines how the crystal decides to pack. In the Ni case the ClO_4^- ions align exactly with the threefold axis while in the Fe case they do not. The value of $a = b = 10.225(3)$ Å is substantially smaller for the Ni complex than the corresponding value of 10.281(2) Å for the Fe complex but the volume per formula unit is larger for the Ni complex.

Results and discussion

Properties of the tris(ligand) complexes $[FeL_3]^{2+}$ and $[NiL_3]^{2+}$

The deep red $[FeL_3]^{2+}$ ion is readily formed by interaction of L with iron(II) salts in either water or ethanol and can be isolated as the sparingly soluble perchlorate or fluoroborate salts. It is low spin, as expected. The magnetic moment of the complex perchlorate is 0.7 BM at 298 K and this shows no significant increase at least up to 333 K (Table 2). This value is normal for singlet state Fe(II). The electronic spectrum of the complex is typical for the iron(II) di-imine chromophore and the maximum absorption occurs at 19 200 cm^{-1} in acetone solution ($\epsilon = 14\,000$ l mol^{-1} cm^{-1}), this being at almost the same frequency as the similar absorption in the spectrum of $[Fe(bipy)_3]^{2+}$ [21], but somewhat lower than that for $[Febpz)_3]^{2+}$ [22] (bpz is 2,2'-bipyrazinyl, which is isomeric with L). The absorption is assigned to a $t_2 \rightarrow \pi^*$ charge transfer transition.

TABLE 2. Magnetic data for complexes

T (K)	$10^{10} \times \chi_M$ (m^3 mol^{-1})	μ_{eff} (BM)
$[FeL_3][ClO_4]_2$ (solid)		
303	28	0.74
313	28	0.75
323	28	0.76
$[FeL_3][FeCl_4]_2$ (solid)		
89	3890	4.70
128	2740	4.72
176	2010	4.75
225	1600	4.79
275	1320	4.81
295	1220	4.78
313	1150	4.79
$[NiL]_3[ClO_4]_2H_2O$ (solid)		
89	1530	2.94
109	1280	2.97
128	1100	2.99
225	640	3.04
275	530	3.05
313	480	3.11
$[CoL_3][BF_4]_2$ (solid)		
89	600	1.85
109	500	1.87
128	450	1.91
152	390	1.94
176	360	2.02
201	330	2.06
225	310	2.11
250	320	2.24
275	330	2.39
295	330	2.48
313	330	2.58
333	350	2.72
353	360	2.85
373	380	3.00
383	380	3.06
$[FeL_3][FeCl_4]0.5H_2O$ (solid)		
89	2150	3.49
128	1510	3.51
176	1100	3.51
225	850	3.49
275	690	3.48
304	630	3.49
333	570	3.49
363	530	3.49
373	520	3.51
$[FeL_2(NCS)_2]$ (solid)		
89	600	1.85
128	430	1.87
176	320	1.91
225	245	1.87
275	200	1.86
304	175	1.84
$[CoL_3][ClO_4]_20.5H_2O$ (solid)		
89	570	1.80
128	420	1.86
176	340	1.95
225	280	1.99
275	260	2.14
295	250	2.18
323	250	2.28
$[CoL_3][ClO_4]_2$ (aqueous solution)		
300	280	2.31
320	290	2.43
328	300	2.51
333	320	2.60

The absorption band is unsymmetrical, with a shoulder on the high-energy side but this is not as well-defined as is frequently observed for iron(II) diimine systems [23].

The Mössbauer spectrum of $[FeL_3][BF_3]_2$ is similar to that of $[Fe(bipy)_3][ClO_4]_2$ [24], showing a single doublet with relatively small quadrupole splitting. The isomer shift for $[FeL_3][BF_4]_2$ (Table 3) is significantly less than that for $[Fe(bipy)_3][ClO_4]_2$ and this is indicative of increased d_π–p_π character to the metal–ligand interaction, consistent with the observations of Ernst and Kaim [6]. Also consistent with this is the relatively strong stabilisation, with respect to oxidation, of iron(II) in the bipyridazine complex. The cyclic voltammogram for the complex in either 1 M H^+ (H_2SO_4) or in acetonitrile solution reveals a reversible one-electron redox change within the scanning range 0.6–1.8 V versus SCE, and leads to values for the $[FeL_3]^{3+}/[FeL_3]^{2+}$ couple of 1.33 and 1.58 V (versus the normal hydrogen electrode) in the two media, respectively. The corresponding potential for the $[Fe(phen_3]^{3+}/[Fe(phen)_3]^{2+}$ couple measured in 1.0 M H^+ (H_2SO_4) under the same experimental conditions was found to be 1.04 V.

Bis(ligand) iron complexes

Because of the particular structural features of L considerable effort was devoted to the attempted preparation of bis(ligand) complexes $[FeL_2X_2]$ since it seemed feasible that these may adopt a *trans* configuration. The preferential formation of the tris(ligand) complex was evident in most instances, however. Thus all attempts at preparation of $[FeL_2Cl_2]$ failed and the species $[FeL_3][FeCl_4]$ was obtained. This presumably contains the tetrahedral $[FeCl_4]^{2-}$ ion, both the magnetic and Mössbauer spectral data being indicative of this. Thus the magnetic moment observed (per iron atom) shows only minor temperature dependence (Table 2) and may be rationalised as an average contribution from L.S. iron(II) in the cation ($\mu = 0.7$ BM) and H.S. iron(II) in the anion ($\mu = 4.9$ BM) (calculated average $\mu = 3.5$ BM), the slightly low value possibly indicating some interaction involving the anionic species. Direct support for the proposed formulation is provided by the Mössbauer spectrum (Fig. 1) which shows clearly the presence of two iron sites. Two doublets are observed in the spectrum, the more intense being associated with the L.S. cation and having parameters (Table 3) very similar to those of the tris(ligand) complex perchlorate. The second, and weaker, doublet is associated with the complex anion and has parameters indicative of high-spin iron(II). These parameters are in fact very similar to those observed

TABLE 3. Mössbauer spectral parameters for iron complexes

Compound	T (K)	Spin state	ΔE_Q[a] (mm s^{-1})	$\delta_{i.s.}$[a, b] (mm s^{-1})
$[FeL_3][ClO_4]_2$	77	$^1A_1$	0.52	0.16
$[FeL_3][BF_4]_2$	77	$^1A_1$	0.56	0.14
$[FeL_2(NCS)_2]$	77	$^1A_1$	0.71	0.29
$[FeL_3][FeCl_4]_2$	77	$^1A_1$	0.55	0.21
$[FeL_3][FeCl_4]_2$	77	$^6A_1$	0.29	0.22
$[FeL_3][Fe(NCS)_4]$	77	$^1A_1$	0.50	0.23
$[FeL_3][Fe(NCS)_4]$	77	$^5T_2$	2.60	1.11
$[FeL_3][FeCl_4]$	77	$^1A_1$	0.55	0.24
$[FeL_3][FeCl_4]$	77	$^5T_2$	3.01	1.11

[a]Estimated error ±0.02. [b]With respect to natural iron.

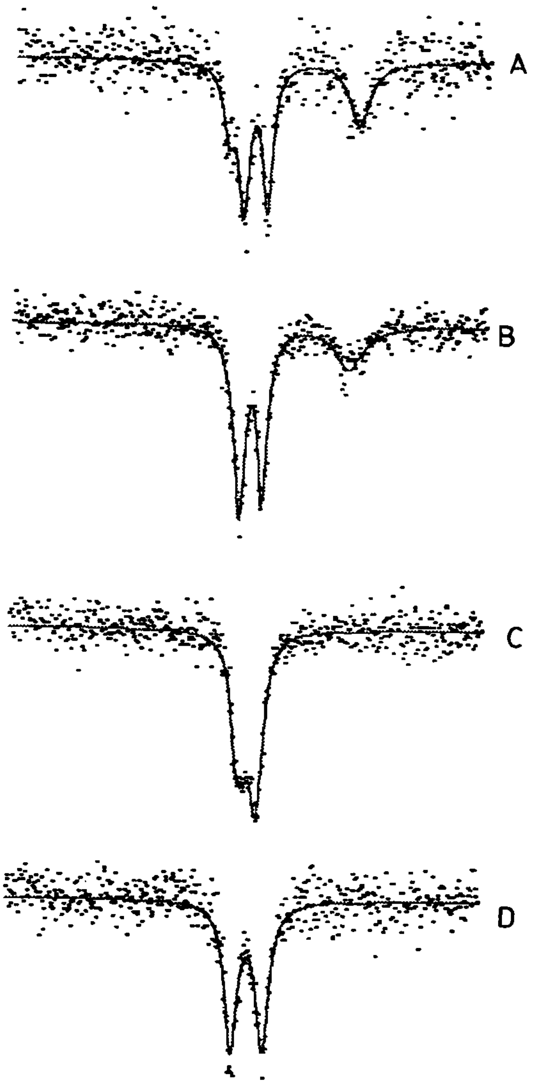

Fig. 1. Mössbauer spectrum at 77 K of: A, $[FeL_3][FeCl_4]$; B, $[FeL_3][Fe(NCS)_4]$; C, $[FeL_3][FeCl_4]_2$; D, $[FeL_2(NCS)_2]$.

for the anion in $[Fe(trpy)_2][FeCl_4]$ at 80 K [25]. The unequal contributions of the two iron species to the Mössbauer spectrum must be associated with a smaller recoil-free fraction for the high-spin species, and hence a reduced Debye–Waller factor. This behaviour is not unusual. A complex of similar stoicheiometry $[FeL_3][Fe(NCS)_4]$ was obtained in attempts to prepare $[FeL_2(NCS)_2]$ by the extraction technique [26] applicable to the preparation of $[Fe(phen)_2(NCS)_2]$. Again the magnetism and the Mössbauer spectrum are consistent with the two different spin states and geometries being present. The Mössbauer parameters assigned to the high-spin species are comparable to those reported for the simple salt $[NMe_4]_2[Fe(NCS)_4]$ [27] and for those in species where the anion is associated with a low-spin iron(II) complex cation [28].

The bis(ligand) iron(II) complex $[FeL_2(NCS)_2]$ was obtained successfully by interaction of iron(II) thiocyanate with the ligand in ethanol when it was obtained as a black crystalline solid. The preparation had to be carried out at room temperature or below to avoid the formation of $[FeL_3][Fe(NCS)_4]$. $[FeL_2(NCS)_2]$ has a low magnetic moment which indicates almost complete spin pairing (Table 2). There is no clear evidence for high-spin material in the Mössbauer spectrum (Fig. 1) but the asymmetry in the peaks due to low-spin species may result from partial overlap with one component of a high-spin doublet (note this asymmetry is not evident in the 'fitted' spectrum since constraints were applied). The moment is essentially temperature-independent, up to 304 K. Above this temperature it increases significantly (up to about 2.3 BM at 383 K), but this change is irreversible. There is an accompanying change in colour and the nature of this indicates that the tris(ligand) complex is being formed and hence a partial rearrangement to $[FeL_3][Fe(NCS)_2]$ is believed to occur. The low-spin nature of $[FeL_2(NCS)_2]$ is unusual, but is another manifestation of the particularly high field strength of **2**. It is usual that bis(thiocyanato)bis(di-imine)iron(II) and related species are either purely high spin or display a temperature-induced singlet ⇄ quintet transition [29] but there are one or two examples of such species that are low spin, e.g. $[Fe(btz)_2(NCSe)_2]$ where btz is 2,2'-bi-4,5-dihydrothiazine [30].

The question does arise as to whether the thiocyanato groups in $[FeL_2(NCS)_2]$ are in *cis* or *trans* positions. The only instance where the *trans* configuration is adopted in a complex of this kind appears to be bis(thiocyanato)bis(4,4'-bi-1,2,4-triazole)-iron(II) [31]. In this complex the *trans* structure was assigned on the basis of the crystal structure determination of the corresponding isostructural cobalt(II) complex. In the absence of X-ray structural information, infrared spectral data can be helpful in the assignment of structures to these kinds of complexes. In perfect *trans* symmetry, the asymmetric CN stretch of the thiocyanato group is infrared active and the symmetric stretch is observable only in the Raman spectra. In the spectrum of bis(thiocyanato)bis(4,4'-bi-1,2,4-triazole)iron(II) a very small splitting (18 cm^{-1}) is observed for the CN stretch [32] and in that for *trans*-$[Ru(bpy)_2(NCS)_2]$ a single band in this region is observed [33]. In the infrared spectrum of $[Fe(bpy)_2(NCS)_2]$, which is known to have the *cis* configuration in the solid [34], two CN absorptions are observed at 2068 and 2061 cm^{-1} at room temperature when the complex is high spin and at about 2100 and 2065 cm^{-1} (depending on the actual polymorph) at low temperature when the complex is essentially low spin [35]. The spectrum of $[FeL_2(NCS)_2]$ in the 2100 cm^{-1} region is similar to that of singlet state $[Fe(bpy)_2(NCS)_2]$ and shows two bands at 2119 and 2050 cm^{-1}. This large splitting is taken as evidence that the thiocyanato groups are in *cis* positions. Bands due to the metal–nitrogen stretching frequencies of the complex were observed in the far infrared region. A strong band at 486 cm^{-1} is assigned to the Fe–N(NCS) stretch and one at 374 cm^{-1} as Fe–N(bipyridazine) stretch. These values are close to those assigned to the analogous bonds in the spectrum of singlet state $[Fe(bpy)_2(NCS)_2]$ on the basis of isotopic substitution studies [36].

Interaction of either bipyridine or phenanthroline with iron(III) chloride in ethanol or acetone leads to the formation of *cis*-bis(ligand) cationic species $[FeL_2Cl_2]^+$ which crystallise as salts of the iron(III) anionic system $[FeCl_4]^-$ [37], and it was thought that this reaction may lead to a corresponding *trans* derivative of **2**. Under the same conditions interaction of **2** with iron(III) chloride led to the spontaneous reduction of iron to iron(II) as $[FeL_3]^{2+}$ and crystallisation of the mixed-valence iron(II)/iron(III) salt $[FeL_3][FeCl_4]_2$. This formulation is supported by the value of the magnetic moment per iron atom which is consistent with the presence of low-spin iron(II) ($\mu = 0.7$ BM) and high-spin iron(III) ($\mu = 5.9$ BM) in the ratio 1:2 (calculated 4.83 BM). The Mössbauer spectrum (Fig. 1) clearly shows contributions from more than one kind of iron centre and can in fact be resolved into two doublets, each with small quadrupole splitting and small isomer shift values. The parameters listed in Table 3 are consistent with the proposed formulation, those for the anionic species being comparable with those obtained for 'simple' derivatives of $[FeCl_4]^-$ [38].

Properties of the tris(ligand)cobalt(II) complexes

Salts of $[CoL_3]^{2+}$ have strongly temperature-dependent magnetic moments which are associated with a temperature-induced doublet $\rightleftarrows$ quartet spin transition. Transitions of this kind are well established for cobalt(II) but they are generally obtained for complexes in which a strong field tridentate group is coordinated to the metal, the classic system being the bis(terpyridine)cobalt(II) ion [39]. Figgins and Busch [40] have pointed out that the tetragonal distortion imposed by the coordination of a conjugated tridentate system will favour the low-spin configuration for cobalt(II) since it is subject to a Jahn–Teller distortion. The first instance of a bidentate chelate group being able to generate the crossover situation for cobalt(II) would seem to be biacetyl-bis-methylimine [41] and few examples have been reported since. The tris(bipyridine)cobalt(II) ion is high spin and shows no unusual temperature-dependence of its magnetism. The field strength in this bipyridine complex must be rather close to that at the doublet (^2E_g) $\rightleftarrows$ quartet ($^4T_{2g}$) crossover for cobalt(II), however, since a transition has been identified from electron paramagnetic resonance studies of the ion trapped in the cavities of a zeolite structure [42]. It is then not surprising that **2**, which provides a stronger field than bpy, can effect a transition in its $[CoN_6]^{2+}$ complex under normal conditions.

The transitions observed in $[CoL_3]X_2$ ($X = ClO_4$; BF_4) are of the continuous kind as are most others reported for cobalt(II) systems and the transition to high-spin species is obviously incomplete at the upper limit of the experimental temperature ranges (Table 2).

In aqueous solution, as in the solid state, $[CoL_3][BF_4]_2$ has magnetic properties which indicate a strong favouring of the doublet (low-spin) state. At room temperature the complex is virtually entirely low spin and has a magnetic moment of 2.3 BM but this is slightly temperature dependent ($\mu = 2.6$ BM at 333 K) indicating thermal population of the quartet state. The diffuse reflectance spectrum of solid $[CoL_3][BF_4]_2$ at 363 and 100 K is shown in Fig. 2 and it can be seen that at the lower temperature there is an increase in intensity of the principal bands at 13 200 and 19 000 cm^{-1}. It is likely that the first band arises primarily from a component of the ligand field $^2E_g \rightarrow {}^2T_{2g}$ transition and the second from a charge-transfer transition. In the spectrum measured for a solution (1.5×10^{-4} M) of the complex in acetone the principal band is at 20 000 cm^{-1} and its intensity ($\epsilon = 3000$ l mol^{-1} cm^{-1}) strongly supports the assignment to charge transfer. The spectral pattern for the solid is similar to that for salts of $[Co(trpy)_2]^{2+}$ in the same range [39].

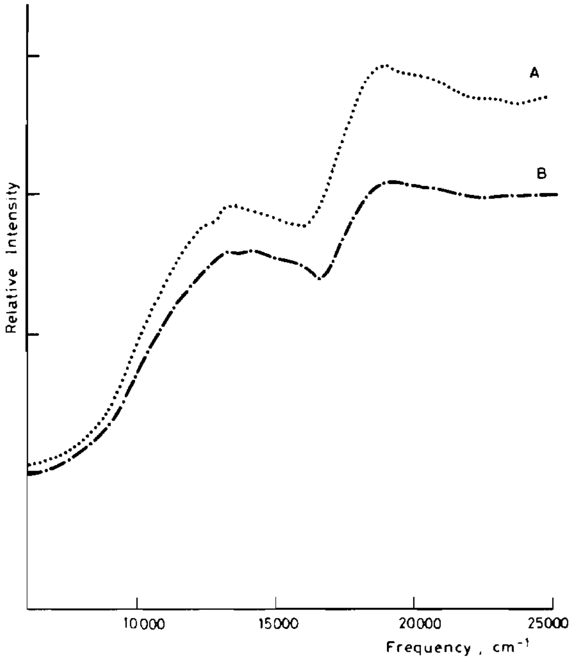

Fig. 2. Diffuse reflectance spectrum of $[CoL_3][BF_4]_2$ at: A, 100 K; B, 363 K.

TABLE 4. Interatomic distances (Å) for $[ML_3][ClO_4]_2$ (M = Fe, Ni)

Atoms	M = Fe	M = Ni
M–N1	1.927(3)	2.060(7)
N2–N1	1.343(5)	1.365(9)
C1–N2	1.329(6)	1.310(11)
C2–C1	1.363(7)	1.416(18)
C3–C2	1.377(7)	1.396(10)
C4–N1	1.342(5)	1.313(13)
C4–C3	1.381(6)	1.349(14)
C4–C4[a]	1.479(9)	1.534(16)

[a] $x-y$, $-y$, $\frac{1}{2}-z$ (M = Fe); $x-y$, $-y$, $-z$ (M = Ni).

The field strength of 2

The properties of the iron(II) and cobalt(II) complexes above all point to a field strength for **2** unusually high for a di-imine type ligand. This was confirmed from the electronic spectral properties of $[NiL_3]^{2+}$. The spectrum of $[NiL_3][ClO_4]_2$ both in the solid state and in solution shows the ligand field transition ν_1 ($^3A_{2g} \rightarrow {}^3T_{2g}$) at 13 200 cm^{-1} ($\epsilon = 16$ l mol^{-1} cm^2). Charge transfer absorption masks the other ligand field bands. The position of ν_1 is at remarkably high energy for a $[NiN_6]^{2+}$ species containing a di-imine system, significantly higher than for $[Ni(bpy)_3]^{2+}$ (12 650 cm^{-1}) [43], and leads to a value of 1320 cm^{-1} for the ligand field parameter $Dq_{Ni^{2+}}$. The magnetism of $[NiL_3][ClO_4]_2$ is normal for Ni(II) in an essentially octahedral field (Table 2).

TABLE 5. Bond angles (°) for $[ML_3][ClO_4]_2$ (M = Fe, Ni)

Atoms	M = Fe	M = Ni
N1–M–N1^{b}	93.5(1)	93.5(2)
N1–M–N1^{c}	92.1(1)	97.3(2)
N1–M–N1^{d}	172.6(2)	166.1(3)
N1–M–N1^{a}	81.3(2)	77.2(4)
M–N1–N2	122.7(3)	121.9(6)
M–N1–C4	116.7(3)	118.0(5)
N2–N1–C4	120.4(4)	119.7(8)
N1–N2–C1	117.2(4)	118.5(10)
N2–C1–C2	124.9(5)	123.3(9)
C1–C2–C3	118.3(5)	116.8(12)
C2–C3–C4	116.0(5)	116.6(13)
N1–C4–C3	123.3(4)	125.1(7)
N1–C4–C4^{a}	112.5(2)	113.1(5)
C3–C4–C4^{a}	124.3(3)	121.8(6)

[a] $x-y, -y, \frac{1}{2}-z$ (M = Fe); $x-y, -y, -z$ (M = Ni). [b] $-y, x-y, z$ (M = Fe); $-y, x-y, z$ (M = Ni). [c] $y, x, \frac{1}{2}-z$ (M = Fe); $y, x, -z$ (M = Ni). [d] $-x, -x+y, \frac{1}{2}-z$ (M = Fe); $-x, -x+y, -z$ (M = Ni).

TABLE 6. Positional parameters for $[FeL_3][ClO_4]_2$

Atom	x	y	z
Fe	0.0000(0)	0.0000(0)	0.25000(0)
N1	0.1815(4)	0.0786(3)	0.3157(2)
N2	0.2018(5)	0.1551(4)	0.3877(2)
C1	0.3259(6)	0.1920(5)	0.4314(3)
C2	0.4333(6)	0.1581(6)	0.4084(3)
C3	0.4133(5)	0.0798(5)	0.3346(3)
C4	0.2838(5)	0.0424(3)	0.2901(2)
Cl1	0.6677(13)	0.3518(10)	0.6383(1)
O1	0.5829(22)	0.3290(25)	0.5695(6)
O2	0.7864(16)	0.3369(16)	0.6181(9)
O3	0.7157(18)	0.4907(15)	0.6681(12)
O4	0.5857(19)	0.2505(19)	0.6976(10)
Cl1′	0.6897(93)	0.3012(94)	0.6338(32)
O1′	0.656(22)	0.339(19)	0.7084(37)
O2′	0.832(10)	0.328(16)	0.636(12)
O3′	0.596(13)	0.155(10)	0.619(12)
O4′	0.675(21)	0.383(17)	0.5725(45)
H(C1)	0.3424	0.2490	0.4849
H(C2)	0.5240	0.1903	0.4444
H(C3)	0.4885	0.0518	0.3139

Primes indicate the minor disordered component.

Structure of tris(ligand)iron and nickel complexes of 2

Because of the unusually high field strength of 2 it was considered desirable to obtain some structural information which would quantify its interaction with metal ions in terms of the actual metal–donor atom distances and possibly offer some structural basis for its high field nature. Accordingly the structures of both $[FeL_3][ClO_4]_2$ and $[NiL_3][ClO_4]_2$ were determined, these being taken as typical for derivatives of first transition series metals in a low-spin (Fe(II))

TABLE 7. Positional parameters for $[NiL_3][ClO_4]_2$

Atom	x	y	z
Ni	0.0000(0)	0.0000(0)	0.0000(0)
N1	0.1937(8)	0.0725(6)	0.1384(6)
N2	0.2118(8)	0.1396(7)	0.2899(6)
C1	0.3300(11)	0.1670(12)	0.3792(9)
C2	0.4399(15)	0.1304(12)	0.3264(14)
C3	0.4179(13)	0.0619(9)	0.1710(12)
C4	0.2938(11)	0.0372(5)	0.0861(9)
Cl	0.3333(0)	0.6667(0)	0.2574(9)
O1	0.3333(0)	0.6667(0)	0.0903(10)
O2	0.2200(12)	0.6858(15)	0.3132(11)
Ni′	0.0000(0)	0.0000(0)	0.5000(0)
N1′	0.1937(8)	0.725(6)	0.3616(6)
N2′	0.2118(8)	0.1396(7)	0.2101(6)
C1′	0.3300(11)	0.1670(12)	0.1208(9)
C2′	0.4399(15)	0.1304(12)	0.1736(14)
C3′	0.4179(13)	0.0619(9)	0.3290(12)
C4′	0.2938(11)	0.0372(5)	0.4139(9)
Cl′	0.3333(0)	0.6667(0)	0.2426(9)
O1′	0.3333(0)	0.6667(0)	0.4097(10)
O2′	0.2200(12)	0.6858(15)	0.1868(11)
H(C1)	0.3436	0.2159	0.4897
H(C2)	0.5287	0.1524	0.3972
H(C3)	0.4902	0.0326	0.1255
H(C1′)	0.3436	0.2159	0.0103
H(C2′)	0.5287	0.1524	0.1028
H(C3′)	0.4902	0.0326	0.3745

Primes indicate the second of the disordered components.

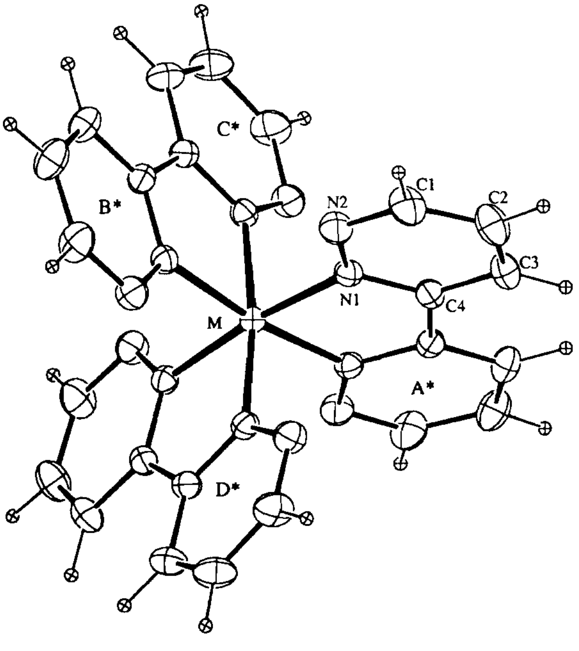

Fig. 3. View of the cation in $[ML_3][ClO_4]_2$ (M = Fe, Ni) showing the atom labelling scheme.

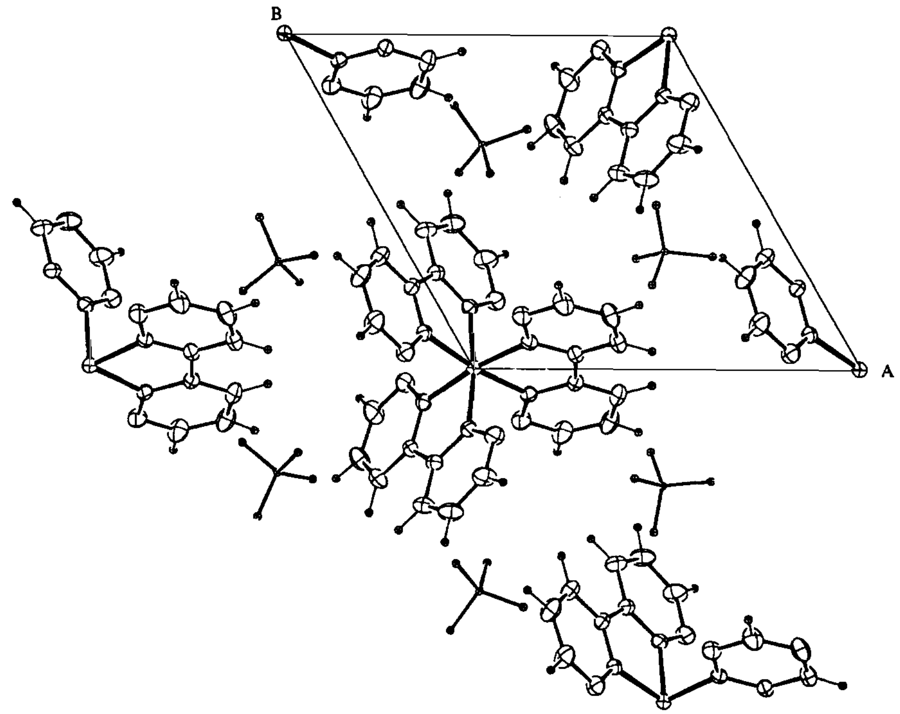

Fig. 4. Unit cell packing diagram for $[ML_3][ClO_4]_2$ (M = Fe, Ni).

or high-spin (Ni(II)) configuration. Bond lengths and selected bond angles for the complexes are shown in Tables 4 and 5, respectively. Positional parameters are listed in Tables 6 and 7. Figure 3 is a view of $[ML_3]^{2+}$ (M = Fe, Ni) and shows the labelling scheme used for the atoms in both structures.

The two crystal structures are almost identical, their unit cells (Fig. 4) have similar *a* and *b* dimensions (Table 1) but the *c* axis for the Fe(II) complex ($Z = 2$) is approximately twice that of the Ni complex ($Z = 1$). Disorder in the anion orientations for both complexes as well as twinning in the crystal of the nickel complex introduced complications into the structure determinations. The procedures followed to resolve these problems and to refine the structures are detailed in 'Experimental'.

In both complexes, the ligand functions as a bidentate chelate, coordinating through two nitrogen (N1) atoms with M–N distances of 1.927(3) Å for Fe(II) and 2.060(7) Å for Ni(II). These distances are relatively short compared to the average M–N distance in $M(bpy)_3^{2+}$ (1.956(8) Å for Fe(II) [44] and 2.089(5) Å for Ni(II) [45]) and are consistent with the stronger ligand field of L. The bond length data for the nickel complexes of **2** and bpy allow an assessment of the relationship between the field strength and bond distance [46] which has been verified for only a few systems, most notably the high-spin and low-spin forms of $[Fe(bpy)_2(NCS)_2]$ [34].

$$\frac{Dq_{Ni^{2+}}(L)}{Dq_{Ni^{2+}}(bpy)} = \left(\frac{d\text{Ni–N}_{(bpy)}}{d\text{Ni–N}_{(L)}}\right)^5$$

Applying the experimental data it is found that the *Dq* ratio is 1.043 and the distance ratio is within the range 1.042–1.10 (this range being determined by the errors involved in the nickel–nitrogen distances). In view of the significantly different nature (in this context) of the ligands which will have an influence on the relative field strengths, it is gratifying that this shows there is a reasonable correlation between the bond distances and the field strength.

In the refinement of the structures the pyridazine rings were constrained to planarity but the two rings of each bidentate group were not constrained to coplanarity. In fact significant N1A*–C4A*–C4–N1 torsional angles are observed in both the iron and nickel complexes (6.5 and 9.6°, respectively) but these are comparable to the corresponding angles found for the bipyridine complexes. The angles about the metal atoms in the bipyridazine complexes are also fairly close to those in the bipyridine complexes. The ligand 'bite' angles are remarkably similar and the actual ligand 'bite' (*b*), as defined by Kepert and co-workers [3] is also similar for the two ligand systems. For $[FeL_3]^{2+}$ and $[Fe(bpy)_3]^{2+}$ *b* is 1.30 and 1.31 [44], respectively, and for $[NiL_3]^{3+}$ and $[Ni(bpy)_3]^{2+}$ b is 1.25 and 1.27 [45], respectively. The shortest inter-ligand N2–N2 distance (3.3 Å in both $[FeL_3]^{2+}$ and $[NiL_3]^{2+}$) is much shorter than the corresponding C1–C1 (the atoms in the 6 or 6′-positions of bipyridine) distances in complexes of bpy (3.5 Å for both $[Fe(bpy)_3]^{2+}$ and $[Ni(bpy)_3]^{2+}$). This certainly supports the view that inter-ligand repulsive interactions are present in the tris(bipyridine) complexes and these arise, at least in part, from the hydrogen atoms at the 6- and 6′-positions.

The stereochemistry about the metal atom in $[ML_3]^{2+}$ is trigonally distorted from octahedral. The trigonal twist angle (θ) is 25.4° for the Fe(II) complex and 21.7° for the Ni(II) complex ($\theta = 30°$ for true octahedral coordination). The values calculated from the empirical relationship derived by Kepert and coworkers [3] are 24.2 and 21.9°, respectively. The agreement between observed and 'calculated' twist angles is rather better for both bipyridazine complexes than for the corresponding bipyridine complexes and this supports Kepert's proposal that the deviation towards the octahedral limit for the twist angle observed for tris(bipyridine) complexes arises from the steric interaction of the hydrogen atoms at the 6- and 6′-positions in one ligand molecule with those of a second. The reduction of this interaction in the complexes of bipyridazine no doubt accounts in part for the remarkably high field strength of the ligand.

Supplementary material

Tables of thermal parameters, torsional angles and structure factors for the structures of $[ML_3][ClO_4]_2$ and analytical data for all the complexes are available from the authors.

Acknowledgements

D.O. is grateful for an Australian Development Assistance Bureau Award. Appreciation is expressed to Dr P. Pham for the microanalytical data and to Mr D. C. Craig for the collection of the diffraction data. Financial support from the Australian Research Council is gratefully acknowledged.

References

1 E. D. McKenzie, *Coord. Chem. Rev.*, *6* (1971) 187.

2 H. Nagao, H. Nishimura, H. Funato, H. Y. Ichikawa, F. S. Howell, M. Mukaida and H. Kakihana, *Inorg. Chem.*, *28* (1989) 3955.

3 H. A. Goodwin, D. L. Kepert, J. M. Patrick, B. W. Skelton and A. H. White, *Aust. J. Chem.*, *37* (1984) 1817.

4 J. F. Lafferty and F. H. Case, *J. Org. Chem.*, *32* (1967) 1591.

5 R. D. Gillard, D. W. Knight and P. A. Williams, *Transition Met. Chem.*, *5* (1980) 321.

6 S. Ernst and W. Kaim, *J. Am. Chem. Soc.*, *108* (1986) 3578.

7 H. Igeta, T. Tsuchiya, M. Nakajima and H. Yokogawa, *Tetrahedron Lett.*, *28* (1969) 2359.

8 H. Igeta, T. Tsuchiya, M. Nakajima and H. Yokogawa, *Chem. Pharm. Bull.*, *18* (1970) 1228.

9 M. Tiecco, L. Testaferri, M. Tingoli, D. Chianelli and M. Montanucci, *Synthesis*, *9* (1984) 736.

10 R. C. Evans and F. Y. Wiselogle, *J. Am. Chem. Soc.*, *67* (1945) 60.

11 C. Grundmann, *Chem. Ber.*, *81* (1948) 1.

12 B. N. Figgis and J. Lewis, in J. Lewis and R. G. Wilkins (eds.), *Modern Coordination Chemistry*, Interscience, New York, 1960, p. 400.

13 D. F. Evans, *J. Chem. Soc.*, (1959) 2003.

14 M. V. Baker, L. D. Field and T. W. Hambley, *Inorg. Chem.*, *27* (1988) 2872.

15 J. A. Ibers and W. C. Hamilton (eds.), *International Tables for X-Ray Crystallography*, Vol. 4, Kynoch Press, Birmingham, U.K., 1974.

16 P. Main, *MULTAN 80*, University of York, U.K., 1980.

17 A. D. Rae, *RAELS*, University of New South Wales, Australia, 1986–1988.

18 C. K. Johnson, *ORTEP-II*, Oak Ridge National Laboratory, TN, U.S.A., 1976.

19 A. D. Rae, *Acta Crystallogr., Sect. A*, *31* (1975) 560.

20 A. D. Rae and A. T. Baker, *Conf. Abstr.*, American Crystallographic Association, Hamilton, 1986, Paper PA 25.

21 C. K. Jørgensen, *Acta Chem. Scand.*, *11* (1957) 166.

22 A. B. P. Lever, J. Lewis and R. S. Nyholm, *J. Chem. Soc.*, (1964) 1187.

23 P. Krumholz, *J. Am. Chem. Soc.*, *75* (1953) 2163.

24 R. L. Collins, R. Pettit and W. A. Baker, Jr., *J. Inorg. Nucl. Chem.*, *28* (1966) 1001.

25 W. M. Reiff, N. E. Erickson and W. A. Baker, Jr., *Inorg. Chem.*, *8* (1969) 2019.

26 P. Ganguli, P. Gütlich and W. Müller, *J. Chem. Soc., Dalton Trans.*, (1981) 441.

27 P. R. Edwards, C. E. Johnson and R. J. P. Williams, *J. Chem. Phys.*, *47* (1967) 2074.

28 H. A. Goodwin, F. E. Smith, E. König and G. Ritter, *Aust. J. Chem.*, *26* (1973) 521.

29 P. Gütlich, *Struct. Bonding (Berlin)*, *44* (1981) 83.

30 G. Bradley, V. McKee, S. M. Nelson and J. Nelson, *J. Chem. Soc., Dalton Trans.*, (1978) 522.

31 W. Vreugdenhil, S. Gorter, J. G. Haasnoot and J. Reedijk, *Polyhedron*, *4* (1985) 1769.

32 J. G. Haasnoot and W. L. Groeneveld, *Z. Naturforsch.*, *346* (1979) 1500.

33 R. H. Herber and G. Nan, *Inorg. Chem.*, *27* (1988) 2644.

34 E. König and K. J. Watson, *Chem. Phys. Lett.*, *6* (1970) 457.

35 E. König, K. Madeja and K. J. Watson, *J. Am. Chem. Soc.*, *90* (1968) 1146.

36 J. H. Takemoto and B. Hutchinson, *Inorg. Chem.*, *12* (1973) 706.

37 H. J. Goodwin, M. McPartlin and H. A. Goodwin, *Inorg. Chim. Acta*, *25* (1977) L74.

38 P. R. Edwards and C. E. Johnson, *J. Chem. Phys.*, *49* (1968) 211.

39 S. Kremer, W. Henke and D. Reinen, *Inorg. Chem.*, *21* (1982) 3013.

40 P. E. Figgins and D. H. Busch, *J. Phys. Chem.*, *65* (1961) 2236.

41 P. E. Figgins and D. H. Busch, *J. Am. Chem. Soc.*, *82* (1960) 820.

42 K. Mizuno and J. H. Lunsford, *Inorg. Chem.*, *22* (1983) 3484.

43 C. K. Jørgensen, *Acta Chem. Scand.*, *9* (1955) 1362.

44 M. E. Garcia Posse, M. A. Juri, P. J. Aymonino, O. E. Piro, H. A. Negri and E. E. Castellano, *Inorg. Chem.*, *23* (1984) 948.

45 A. J. Finney, M. A. Hitchman, D. L. Kepert,. C. L. Raston, G. L. Rowbottom and A. H. White, *Aust. J. Chem.*, *34* (1981) 2177.

46 M. Gerloch and R. C. Slade, *Ligand Field Parameters*, Cambridge University Press, U.K., 1973, p. 31.